

Field Guide to
**Optical
Levitation and
Levitodynamics**

Galina Nemova

SPIE Field Guides
Volume FG54

J. Scott Tyo, Series Editor

SPIE PRESS
Bellingham, Washington USA

Library of Congress Cataloging-in-Publication Data

Names: Nemova, Galina, author. | SPIE (Society), issuing body.

Title: Field guide to optical levitation and levitodynamics / Galina Nemova.

Description: Bellingham, Washington, USA : SPIE Press, [2024] | Series: SPIE field guides ; volume FG54 | Includes bibliographical references and index.

Identifiers: LCCN 2024026728 | ISBN 9781510679962 (spiral bound) | ISBN 9781510679979 (pdf) | ISBN 9781510679986 (epub)

Subjects: LCSH: Optical levitation. | Micrurgy. | Laser cooling. | Beam dynamics. | Nanoparticles—Optical properties.

Classification: LCC TA1697 .N46 2024 | DDC 620/.5—dc23/eng/20240729

LC record available at <https://lcn.loc.gov/2024026728>

Published by

SPIE

P.O. Box 10

Bellingham, Washington 98227-0010 USA

Phone: 360.676.3290

Fax: 360.647.1445

Email: Books@spie.org

Web: www.spie.org

Copyright © 2024 Society of Photo-Optical Instrumentation Engineers (SPIE)

All rights reserved. No part of this publication may be reproduced or distributed in any form or by any means without written permission of the publisher.

The content of this book reflects the thought of the author. Every effort has been made to publish reliable and accurate information herein, but the publisher is not responsible for the validity of the information or for any outcomes resulting from reliance thereon.

Printed in the United States of America.

First printing 2024.

For updates to this book, visit <http://spie.org> and type “FG54” in the search field.

SPIE.

Table of Contents

| | |
|--|-------------|
| Preface | xii |
| Glossary of Symbols and Acronyms | xiii |
| Introduction | 1 |
| A Short History of Optical Pressure | 2 |
| Classical Approach to Electromagnetic Radiation | 3 |
| Maxwell's Equations | 3 |
| Boundary Conditions | 4 |
| Maxwell's Wave Equation | 5 |
| Electromagnetic Wave Properties | 6 |
| Vector and Scalar Potentials | 7 |
| Gaussian Laser Beams | 8 |
| Gaussian Beam Focusing | 9 |
| Focal Fields | 10 |
| Hermite–Gaussian and Laguerre–Gaussian Modes | 11 |
| Helical Phase Fronts | 12 |
| Angular Momentum of Light | 13 |
| Classical Approach to Light–Particle Interactions | 14 |
| Maxwell's Stress Tensor | 14 |
| Vector Harmonics and Generating Functions | 15 |
| Mie Theory | 16 |
| Mie's Scattering Coefficients | 17 |
| T-Matrix Method | 18 |
| Rayleigh's Approximation of Mie Theory | 19 |
| Clausius–Mossotti Relation | 20 |
| Optical Pressure | 21 |
| Optical Pressure | 21 |
| Ray Optics Regime | 22 |
| Intermediate Regime | 23 |
| Dipole Approximation Regime | 25 |
| Random Processes | 26 |
| Random Processes | 26 |
| Autocorrelation and Cross-Correlation Functions | 27 |
| Wiener–Khinchine Theorem | 28 |

Table of Contents

| | |
|--|-----------|
| Classical Approach to Optical Levitation | 29 |
| Trapping Potential | 29 |
| Langevin Equation | 30 |
| Damping Rate | 31 |
| Center-of-Mass (COM) Temperature | 32 |
| Photophoretic Force | 33 |
| Internal Temperature | 34 |
| Trapping with Laguerre–Gaussian Beams | 35 |
| | |
| Optical Tweezers | 36 |
| Single-Beam Optical Tweezers | 36 |
| Holographic Optical Tweezers | 37 |
| Speckle Optical Tweezers | 38 |
| Optical Trap Calibration | 39 |
| Measurement Geometries of Optical Traps | 40 |
| | |
| Parametric Feedback Cooling | 41 |
| Parametric Feedback Cooling | 41 |
| Theory of Parametric Feedback Cooling | 42 |
| | |
| Principles of Quantum Mechanics: General | 43 |
| Difference between Classical and Quantum Physics | 43 |
| Bohr’s Postulates | 44 |
| Matter Waves | 45 |
| Time-Independent Schrödinger Equation | 46 |
| Time-Dependent Schrödinger Equation | 47 |
| Wavefunction | 48 |
| Equation of Continuity | 49 |
| Eigenvalue Equation | 50 |
| Expectation Values of Operators | 51 |
| Quantum Mechanical Measurements | 52 |
| Matrix Formulation of Quantum Theory | 53 |
| Dirac’s Bra–ket Notation | 54 |
| Unitary Time-Evolution Operator | 55 |
| Schrödinger and Heisenberg Pictures | 56 |
| Interaction or Dirac Picture | 57 |
| General Form of the Uncertainty Principle | 58 |

Table of Contents

| | |
|--|---------------|
| Principles of Quantum Mechanics Directly Applicable to Optical Levitodynamics | 59 |
| Density Operator | 59 |
| Density Matrix | 60 |
| Hilbert and Fock–Liouville Spaces | 61 |
| Time Evolution of the Density Operator | 62 |
| Wigner Function | 63 |
| Composite Quantum Systems | 64 |
| Separable and Entangled States | 65 |
| Open Quantum Systems | 66 |
| Dynamics of Open Systems | 67 |
| Born–Markov Approximation | 68 |
| Super-operators | 69 |
| Rotating Wave Approximation | 70 |
| Quantum Harmonic Oscillators | 71 |
| Quantum Harmonic Oscillators | 71 |
| Quantization of the Electromagnetic Field | 72 |
| The Quantum Langevin Equation | 74 |
| Quantum Langevin Equation | 74 |
| Solution of the Quantum Langevin Equation | 76 |
| The Fabry–Pérot Cavity | 77 |
| The Fabry–Pérot Cavity | 77 |
| Input–Output Theory of Open Quantum Systems | 78 |
| Cavity-Assisted Optomechanical Cooling | 79 |
| Cavity-Assisted Optomechanical Cooling | 79 |
| Cavity-Assisted Cooling Based on Cavity Modes | 80 |
| Cavity-Assisted Cooling Based on Cavity Modes | 80 |
| Cavity-Assisted Cooling Based on Coherent Scattering | 81 |
| Hamiltonian of the System | 81 |
| Electromagnetic Field of the System | 82 |
| Cavity Mode | 83 |
| Interaction Hamiltonian | 84 |

Table of Contents

| | |
|---|------------|
| Self-Interaction Terms of the Hamiltonian | 85 |
| Cross-Interaction Terms of the Hamiltonian | 86 |
| Hamiltonian of a Free Electromagnetic Field | 87 |
| Transformed Hamiltonian | 88 |
| The Master Equation | 89 |
| Hamiltonian of the Master Equation | 90 |
| Recoil Heating | 91 |
| Vibrational Noise | 92 |
| Gas Pressure as a Decoherence Channel | 93 |
| Cooling | 94 |
| Cooling Optimization | 95 |
| Application of Ground-State Laser-Cooled Nanoparticles | 96 |
| Collapse Models | 96 |
| Macroscopic Quantum Superpositions | 97 |
| Ground State and Wavefunction Expansion (Step I) | 98 |
| Double Slit (Step II) | 99 |
| Interference Pattern (Step III) | 100 |
| Near-Field Interferometry of Nanoparticles | 101 |
| Near-Field Interferometry of Nanoparticles | 101 |
| Talbot Effect | 102 |
| Nitrogen-Vacancy Centers in Diamond | 103 |
| Nitrogen-Vacancy Centers in Diamond | 103 |
| Energy Levels of an NV Center | 104 |
| Optically Detected Magnetic Resonance | 105 |
| Optical Trapping of Nanodiamonds with NV Centers | 106 |
| Rotational Quantum Levitodynamics | 107 |
| Rotational Quantum Levitodynamics | 107 |
| 6D Cooling of a Nanoellipsoid (Experiment) | 108 |
| 6D Cooling of a Nanoellipsoid (Theory) | 109 |

Table of Contents

| | |
|---|------------|
| Phonon Lasers | 110 |
| Phonon Lasers | 110 |
| The Master Equation of the Phonon Laser | 111 |
| Phonon Dynamics of the Phonon Laser | 112 |
| Particle Tracking | 113 |
| Particle Tracking | 113 |
| Principle of Signal Detection | 114 |
| Photodetectors | 115 |
| Photon Counting of a Classical Field | 116 |
| Quantum Theory of Detection | 117 |
| Photon Correlation Measurements | 118 |
| Equation Summary | 119 |
| Bibliography of Further Reading | 130 |
| Index | 134 |

A Short History of Optical Pressure

- In 1619, Johannes Kepler hypothesized in his treatise *De Cometi* that light from the Sun exerting pressure was the reason a comet tail always points away from the Sun.
- In 1873, James Clerk Maxwell hypothesized in *A Treatise on Electricity and Magnetism* that electromagnetic radiation is associated with linear momentum. It exerts a pressure on an exposed surface.
- In 1900, Peter Lebedev was the first to measure radiation pressure and announced his findings at a conference in Paris. In 1901, he published two papers “Untersuchungen über die Druckkräfte des Lichtes” and “Опытное исследование светового давления” in leading European and Russian journals. In 1901, the measurement was independently confirmed by Gordon Nichols and Ernest Hull in the paper “A preliminary communication on the pressure of heat and light radiation” in *The Physical Review* journal.
- In 1904, John Henry Poynting, in the paper “Radiation in the solar system: its effect on temperature and its pressure on small bodies,” came up with the idea of the optical manipulation of microscopic particles.
- In 1970, Arthur Ashkin guided particles in water with a weakly focused horizontal laser beam. He observed the acceleration of particles by **radiation force** and the pulling of particles toward the beam axis by **gradient force**.
- In 1971, Arthur Ashkin and Joseph Dziedzic demonstrated optical levitation of dielectric particles in air that relied on the balance between the axial radiation pressure and the gravitational force.
- In 1986, a **single-beam gradient force trap (optical tweezers)** was demonstrated by Arthur Ashkin and his colleagues. This experiment was a breakthrough in the field of optical levitation.
- In 2020, **ground-state cooling** in a room temperature environment was achieved for the first time with a silica nanoparticle using cavity cooling by **coherent scattering**.

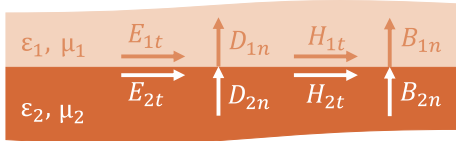
Boundary Conditions

Using the theorems of Gauss and Stokes, one can obtain Maxwell's equations in integral form:

$$\oint_L \mathbf{H} d\mathbf{l} = \int_S \left(\mathbf{J} + \frac{\partial \mathbf{D}}{\partial t} \right) d\mathbf{S} \qquad \oint_{\tilde{S}} (\mathbf{D} d\mathbf{S}) = \int \rho dV$$

$$\oint_L \mathbf{E} d\mathbf{l} = - \int_S \frac{\partial \mathbf{B}}{\partial t} d\mathbf{S} \qquad \oint_{\tilde{S}} (\mathbf{B} d\mathbf{S}) = 0$$

Here S is any surface bounded by the closed curve L . \tilde{S} is a closed surface. The integral forms of Maxwell's equations lead to the boundary conditions:



- The normal components of the **electric displacement** (D_{2n} and D_{1n}) change abruptly across the surface by an amount equal to the surface charge density $\tilde{\rho}$:

$$D_{2n} - D_{1n} = \tilde{\rho}$$

- The normal components of the **magnetic induction** (B_{2n} and B_{1n}) are continuous across the surface:

$$B_{2n} = B_{1n}$$

- The tangential components of the **electric field strength** (E_{2t} and E_{1t}) are continuous across the surface:

$$E_{2t} = E_{1t}$$

- The tangential components of the **magnetic field strength** (H_{2t} and H_{1t}) change abruptly by an amount equal to the surface current density \tilde{J} :

$$H_{2t} - H_{1t} = \tilde{J}$$

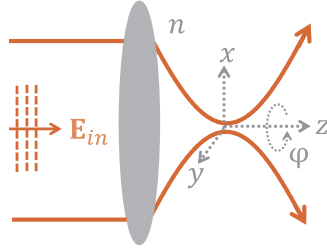
Focal Fields

Consider a Gaussian beam propagating along the z -axis and polarized along the x -axis. Its electric field is

$$\mathbf{E}_{in} = E_{in} \mathbf{e}_x, \text{ where } E_{in} = E_0 \exp\left(\frac{-f^2 \sin^2 \theta}{w_0^2}\right)$$

Let us assume that this beam is incident on a lens with focal length f and **numerical aperture (NA)**

$$NA = n \sin \theta_{max}.$$



The focal field in the cylindrical coordinates has the form

$$\mathbf{E}(r, \varphi, z) = -\frac{ikf}{2} E_0 e^{-ikf} \begin{bmatrix} I_{00} + I_{02} \cos(2\varphi) \\ I_{02} \sin(2\varphi) \\ -2iI_{01} \cos(\varphi) \end{bmatrix},$$

where

$$I_{00} = \int_0^{\theta_{max}} f_w(\theta) (\cos \theta)^{1/2} \sin \theta (1 + \cos \theta) J_0(k\rho \sin \theta) e^{ikz \cos \theta} d\theta$$

$$I_{01} = \int_0^{\theta_{max}} f_w(\theta) (\cos \theta)^{1/2} \sin^2 \theta J_1(k\rho \sin \theta) e^{ikz \cos \theta} d\theta$$

$$I_{02} = \int_0^{\theta_{max}} f_w(\theta) (\cos \theta)^{1/2} \sin \theta (1 - \cos \theta) J_2(k\rho \sin \theta) e^{ikz \cos \theta} d\theta$$

Here J_n is the n^{th} -order Bessel function, and

$$f_w(\theta) = \exp\left(-\frac{1}{f_0^2} \frac{\sin^2 \theta}{\sin^2 \theta_{max}}\right)$$

is the **apodization function**.

Difference between Classical and Quantum Physics

Consider the general principles of quantum mechanics, which will be helpful in understanding the principles of quantum optical levitodynamics.

By the beginning of the 20th century, a physical picture of the world was created, based on Newton's mechanics and Maxwell's electrodynamic theory. However, a number of problems were not explained within the framework of these concepts.

■ The *first* of these problems was the ultraviolet divergence of blackbody radiation, also known as the **ultraviolet catastrophe (UVC)**. Lord Rayleigh and James Jeans considered the behavior of electromagnetic waves within a cavity, which can serve as a blackbody, and used $\kappa_B T$ as the value of the energy per mode, where κ_B is the **Boltzmann constant** and T is the temperature. They obtained the relation, known as the **Rayleigh–Jeans formula**, for the spectral radiance $u(\nu)$ of the blackbody:

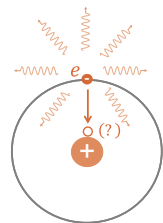
$$u(\nu) = \frac{8\pi\nu^2}{c^3} \kappa_B T$$

where c is the speed of light and ν is the frequency.

At high frequencies ($\nu \rightarrow \infty$), the spectral radiance tends to infinity:

$$u(\nu) \rightarrow \infty (?)$$

■ The *second* problem was connected with **Rutherford's planetary atomic model**, which suggests that electrons spin around a positively charged nucleus in circular orbits. Following Maxwell's theory, the electron moving with acceleration on its circular trajectory must lose its energy due to radiation emission. Finally, it must fall on the nucleus. This problem is called the **radiation collapse** of the classical atomic model.



Dirac's Bra-ket Notation

A **Hermitian operator** expressed in matrix terms must satisfy the equation

$$\hat{O} = \hat{O}^\dagger$$

where

$$\hat{O} = \begin{bmatrix} o_{11} & o_{12} & \cdots \\ o_{21} & o_{22} & \cdots \\ \vdots & \vdots & \ddots \end{bmatrix} \quad \text{and} \quad \hat{O}^\dagger = \begin{bmatrix} o_{11}^* & o_{21}^* & \cdots \\ o_{12}^* & o_{22}^* & \cdots \\ \vdots & \vdots & \ddots \end{bmatrix}$$

The “dagger” character “†” is widely used to indicate the Hermitian adjoint.

In 1939, Paul Dirac introduced a new **bra-ket notation** for quantum states in order to simplify quantum mechanical expressions. The source of this term is the English word “bracket.” For example, a wavefunction expanded in an orthogonal set of eigenfunctions can be written

$$\psi = \sum_n c_n \psi_n \Rightarrow |\psi\rangle = \sum_n c_n |\psi_n\rangle$$

where $|\psi\rangle$ and $|\psi_n\rangle$ are the **ket vectors**:

$$|\psi\rangle = \begin{bmatrix} c_1 \\ c_2 \\ \vdots \end{bmatrix}, \quad |\psi_1\rangle = \begin{bmatrix} 1 \\ 0 \\ \vdots \end{bmatrix}, \quad |\psi_2\rangle = \begin{bmatrix} 0 \\ 1 \\ \vdots \end{bmatrix}, \dots$$

The expansion coefficients are

$$c_m = \langle \psi_m | \psi \rangle$$

The wavefunction ψ^* can be presented by the **bra vector**:

$$\langle \psi | = [c_1^* \quad c_2^* \quad \cdots]$$

The bra vector is the Hermitian adjoint of the ket vector, and vice versa.

The matrix element o_{nm} of the operator \hat{O} can be presented in a bra-ket notation as

$$o_{nm} = \int \psi_n^* \hat{O} \psi_m dV \Rightarrow o_{nm} = \langle \psi_n | \hat{O} | \psi_m \rangle$$

Hilbert and Fock–Liouville Spaces

A **Hilbert space** (\mathcal{H}) is a complex vector space with an inner product $\langle \psi | \varphi \rangle$, like the well-known Cartesian geometrical space. The inner product associates a complex number with any pair of states $|\psi\rangle$ and $|\varphi\rangle$. The Hilbert space is named after David Hilbert, who studied vector spaces with infinite dimensions. Today, the term is often used in a way that includes finite-dimensional spaces.

Any pure state $|\psi\rangle$ can be expanded into a complete orthonormal basis set $|\varphi_n\rangle$ as $|\psi\rangle = \sum_m^{\mathcal{M}} c_m |\varphi_m\rangle$.

There are many possible bases, in which the same vector is represented by different coefficients, but the number \mathcal{M} of basis states required to obtain all vectors is always the same. It is called the dimension of the Hilbert space ($\mathcal{H}_{\mathcal{M}}$).

Let us assume that a system is described by a density operator $\rho = \sum_i p_i |\psi_i\rangle \langle \psi_i|$.

- If $\boxed{Tr(\rho^2) = Tr(\rho) = 1}$, the system is in a **pure state**.
- If $\boxed{Tr(\rho^2) < 1}$, the system is in a **mixed state**.

The quantity $\boxed{Tr(\rho^2)}$ is called the **purity of the state**. It satisfies the inequalities $\frac{1}{\mathcal{M}} \leq Tr(\rho^2) \leq 1$, where \mathcal{M} is the dimension of the Hilbert space.

One can create a linear vector space of density matrices called **Fock–Liouville space** by converting the matrices into vectors ($\rho \rightarrow |\rho\rangle\rangle$). In the case of a two-state system (\mathcal{H}_2),

$$\rho = \begin{bmatrix} \rho_{00} & \rho_{01} \\ \rho_{10} & \rho_{11} \end{bmatrix} \rightarrow |\rho\rangle\rangle = \begin{bmatrix} \rho_{00} \\ \rho_{01} \\ \rho_{10} \\ \rho_{11} \end{bmatrix}$$

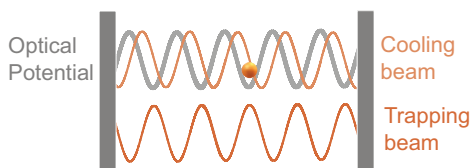
The scalar product of matrices ρ and $\tilde{\rho}$ is defined as

$$\langle\langle \tilde{\rho} | \rho \rangle\rangle = Tr(\tilde{\rho}^\dagger \rho)$$

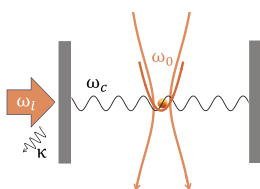
Cavity-Assisted Optomechanical Cooling

In motional cooling of atoms or molecules, their internal structure is involved in the cooling process. In a number of cases, the internal structure of a particle cannot be involved in the cooling process. These schemes include cooling of microparticles and nanoparticles made of solids. In these cases, coupling the motion of a particle to an **optical cavity field** can be used instead of using the internal structure of the particles. Let us consider three schemes.

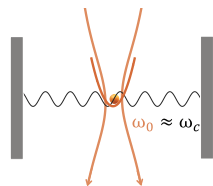
A subwavelength dielectric sphere interacts with two optical modes of a Fabry–Pérot cavity. One resonantly driven mode provides an optical dipole trap for the sphere. The second mode is driven by a weaker “cooling” beam. It has a nonzero intensity gradient at the trap center, which provides a radiation pressure cooling force.



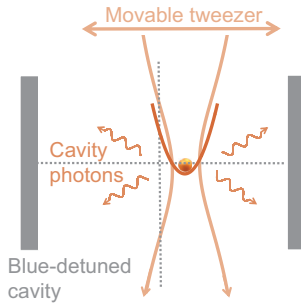
In the second scheme, a particle is trapped by means of optical tweezers inside a high-finesse optical cavity. These optical tweezers create the harmonic potential for the particle. The cavity is driven by blue-detuned ($\Delta = \omega_c - \omega_l = -\omega_0$) laser light. Here ω_c , ω_l , and ω_0 are frequencies of the cavity mode, the cavity driving laser, and the tweezers, respectively. This laser light is responsible for cooling the particle. Laser phase noise can prohibit ground-state cooling at relevant nanoparticle trap frequencies.



A promising alternative is cavity cooling by **coherent scattering** from an optical trapping field. In this case, the particle produces scattering that is coherent with the trap laser. Scattering of these photons in an initially empty blue-detuned cavity provides cooling.



Hamiltonian of the System



Consider cavity cooling by coherent scattering. A particle is trapped at the focus of an optical tweezer propagating along the z -axis at frequency $\omega_0 = 2\pi c/\lambda_0$, where λ_0 is the tweezer wavelength and c is the vacuum speed of light. The particle is coupled to a cavity mode with frequency ω_c . The system can be described by a Hamiltonian,

$$\hat{H} = \frac{\hat{P}^2}{2m} + \hat{H}_f + \hat{H}_{int}$$

containing the kinetic energy of the free particle $\frac{\hat{P}^2}{2m}$ with the center of mass (COM) momentum operator \hat{P} and mass m . The **Hamiltonian** of the free electromagnetic field is

$$\hat{H}_f = \frac{\epsilon_0}{2} \int d^3\mathbf{r} [\hat{\mathbf{E}}^2(\mathbf{r}) + c^2 \hat{\mathbf{B}}^2(\mathbf{r})],$$

where $\hat{\mathbf{E}}$ and $\hat{\mathbf{B}}$ are the electric and magnetic field operators, respectively, and the particle–field interaction term is

$$\hat{H}_{int} = -\frac{1}{2} \alpha \hat{\mathbf{E}}^2(\hat{\mathbf{R}}),$$

where $\hat{\mathbf{R}}$ is the operator of the COM position. The particle polarizability is

$$\alpha = 3\epsilon_0 V \frac{\epsilon - 1}{\epsilon + 2},$$

where V is the volume of the particle with radius $r_p \ll \lambda_0$.

Cooling Optimization

Assume that the cavity is tuned to $\delta' = \Omega'_j$. In this case, the steady-state phonon occupation can have several limits.

I. $\langle \bar{n}_j \rangle_{ss} \approx \frac{\Gamma_j}{\kappa'}$ for $\kappa' \ll |g'_j| \ll \Omega'_j$

In that case, cooling is limited by the small cavity loss. This cavity loss cannot effectively reduce the cavity occupation. This results in an increase in the steady-state phonon occupation.

II. $\langle \bar{n}_j \rangle_{ss} \approx \frac{\kappa' \Gamma_j}{|g'_j|^2}$ for $|g'_j| \ll \kappa' \ll \Omega'_j$

In that case, the low value of the optomechanical coupling is an obstacle to cooling. Cooling becomes inefficient as κ' increases.

III. $\langle \bar{n}_j \rangle_{ss} \approx \frac{2\Gamma_j}{\kappa'}$ for $\kappa' \approx |g'_j| \ll \Omega'_j$

In that case, the cooling process is optimized. The rate at which photons are scattered into the cavity is equal to the rate at which they leave the cavity through the cavity mirrors.

In 2020, *ground-state cooling* in a *room temperature* environment was achieved for the first time. A silica nanoparticle of nominal diameter $D_p = 143 \pm 4$ nm was trapped and cooled in a vacuum chamber using cavity cooling by coherent scattering. The tweezer power in the focus was $P_{tw} \approx 400$ mW at the wavelength $\lambda_0 = 1064$ nm. The particle was placed within an optical cavity (finesse $\mathcal{F} \approx 73000$, linewidth $\kappa/2\pi = 193 \pm 4$ kHz). The tweezer potential provided motional frequencies $(\Omega_x, \Omega_y, \Omega_z)/2\pi = (305, 275, 80)$ kHz. The measured phonon number along the cavity x -axis for the laser detuning $(\omega_c - \omega_0)/2\pi = 315$ kHz was

$$\langle \bar{n}_x \rangle_{ss} = 0.43 \pm 0.03$$

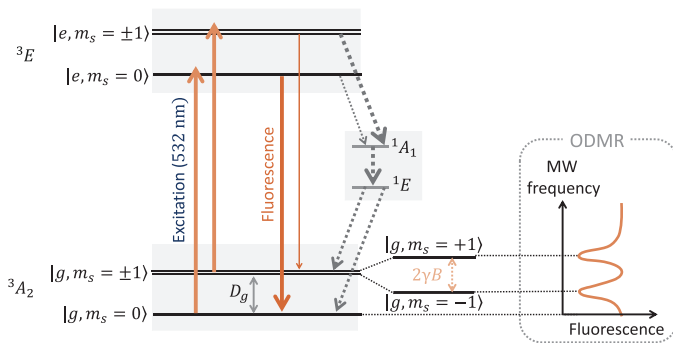
The corresponding temperature of the motion was $T_x \approx 12.2 \pm 2.3$ μ K. The total heating rate was $\Gamma_x/2\pi \approx 20.6 \pm 2.3$ kHz at a pressure of $\sim 10^{-6}$ mbar.

Optically Detected Magnetic Resonance

A microwave (MW) source in the gigahertz range applied to the NV center can cause Rabi oscillations between the $|g, m_s = 0\rangle$ and the $|g, m_s = \pm 1\rangle$ degenerate state with Rabi frequency; these oscillations depend on the amplitude of the applied MW field.

A pump laser (532 nm) applied to the system excites the system to an excited-state triplet 3E from which the system decays radiatively back to the ground-state triplet 3A (with fluorescence in a wavelength range of $\approx 638\text{--}800\text{ nm}$) or nonradiatively through 1A_1 and 1E singlets.

The dependence between the fluorescence intensity and the frequency of the MW source, which is scanned across the ground-state splitting, is called **optically detected magnetic resonance (ODMR)**.



There are different approaches to the ODMR method. The simplest is continuous-wave optically detected magnetic resonance (CW ODMR), in which microwave and laser excitation are applied simultaneously.

- ODMR can be used to estimate D_g .
- ODMR can be used to measure a magnetic field B applied to the system. The applied magnetic field will split the $|g, m_s = \pm 1\rangle$ degenerate state. Dips in fluorescence appear when the MW frequency is resonant with the transitions between $m_s = 0$ and $m_s = \pm 1$.

Principle of Signal Detection

Consider a spherical particle trapped by a Gaussian beam with amplitude E_0 propagating along z and linearly polarized along x in the dipole approximation regime. The respective far fields of the referenced and dipole scattered fields in the paraxial approximation have the forms

$$\mathbf{E}_{ref}^{ff} = E_{ref} \exp[i(kR - \pi/2)] \mathbf{e}_x$$

$$\mathbf{E}_{dip}^{ff} = E_{dip} \exp[i(kR + \phi)] \mathbf{e}_x,$$

where

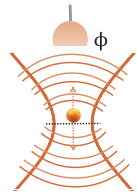
$$\phi = -\mathbf{k} \cdot \mathbf{r}_{dp} + (k - 1/z_0)z_{dp}$$

is the phase modulated by the particle motion $\mathbf{r}_{dp}(t)$, where \mathbf{r}_{dp} is the radius vector of the trapped particle. E_{ref} and E_{dip} are amplitudes. The detector is located a distance R from the focus. At the detector, the fields interfere and produce an intensity distribution proportional to

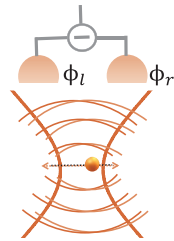
$$I \propto |\mathbf{E}_{ref}^{ff} + \mathbf{E}_{dip}^{ff}|^2 = E_{dp}^2 + 2E_{dp}E_{ref} \sin \phi_{dp} + E_{ref}^2$$

The first term on the right side is small and can be ignored.

■ Let us integrate this relation over the detector area. The x and y dependency vanishes due to the symmetry. The detector output only depends on z . For small displacements z_{dp} , one can get a signal $\propto E_{dp}E_{ref}z_{dp}/z_0$ plus $\propto E_{ref}^2$.



■ For the x_{dp} and y_{dp} displacements of the particle, the beam must be split. The two resulting beams are detected with a balanced detector. The constant term and the dependency on z in the relation for the intensity I are canceled. One can measure a signal $\propto E_{dp}E_{ref}x_{dp}/w_0$ for x and the corresponding signal for y .





Galina Nemova is a research fellow at École Polytechnique de Montréal. After receiving her M.Sc. and Ph.D. degrees from the Moscow Institute of Physics and Technology in 1987 and 1990, respectively, she served as a staff scientific researcher at the Kotelnikov Institute of Radio Engineering and Electronics, Russian Academy of Sciences (1990–2000). She was employed by Laval University (2000–2002) and Bragg Photonics Inc., Québec (2002–2004). In 2004, she joined École Polytechnique de Montréal. Dr. Nemova is a Senior Member of Optica, formerly known as the Optical Society of America (OSA). She has edited three books and authored more than 100 papers. She is the author of *Field Guide to Laser Cooling Methods* (2019) and *Field Guide to Light–Matter Interaction* (2022). Her research interests cover a broad range of photonics topics, including rare-earth–doped materials, nanophotonics, fiber lasers and amplifiers, Raman lasers, nonlinear optics, laser cooling of solids, and quantum optics.